

Temperature dependence of the superconducting proximity effect quantified by scanning tunneling spectroscopy

A. Stepniak,¹ M. Caminale,¹ A. A. Leon Vanegas,¹ H. Oka,¹ D. Sander,^{1,a} and J. Kirschner^{1,2}

¹Max-Planck-Institut für Mikrostrukturphysik, Weinberg 2, 06120 Halle (Saale), Germany

²Institut für Physik, Martin-Luther-Universität Halle-Wittenberg, 06120 Halle (Saale), Germany

(Received 17 November 2014; accepted 13 January 2015; published online 21 January 2015)

Here, we present the first systematic study on the temperature dependence of the extension of the superconducting proximity effect in a 1–2 atomic layer thin metallic film, surrounding a superconducting Pb island. Scanning tunneling microscopy/spectroscopy (STM/STS) measurements reveal the spatial variation of the local density of state on the film from 0.38 up to 1.8 K. In this temperature range the superconductivity of the island is almost unaffected and shows a constant gap of a 1.20 ± 0.03 meV. Using a superconducting Nb-tip a constant value of the proximity length of 17 ± 3 nm at 0.38 and 1.8 K is found. In contrast, experiments with a normal conductive W-tip indicate an apparent decrease of the proximity length with increasing temperature. This result is ascribed to the thermal broadening of the occupation of states of the tip, and it does not reflect an intrinsic temperature dependence of the proximity length. Our tunneling spectroscopy experiments shed fresh light on the fundamental issue of the temperature dependence of the proximity effect for atomic monolayers, where the intrinsic temperature dependence of the proximity effect is comparably weak. © 2015 Author(s). All article content, except where otherwise noted, is licensed under a Creative Commons Attribution 3.0 Unported License. [<http://dx.doi.org/10.1063/1.4906554>]

Recent advances in nanofabrication and nanocharacterization renewed the interest in the so-called superconducting proximity effect due to the possibility to examine this effect at nanoscales.^{1–9} The proximity effect is observed at the junction between a metal (M) and a superconductor (S), and it leads to a depletion of the density of states (DOS) around the Fermi energy in the metal. An induced energy gap in M is therefore observed, and it is the hallmark of the superconducting proximity effect. This electronic feature decays on a characteristic length from the S–M boundary, called proximity length (PL).^{10,11}

Spatial variations of the DOS in the M are accessible experimentally by scanning tunneling microscopy and spectroscopy (STM/STS) with high energy and spatial resolution. This technique has been exploited to study and to visualize the proximity effect in Pb films surrounding superconducting Pb nanoislands on Si(111) substrates.^{6–8}

Thermal energy drives a Cooper pair breaking¹² for the induced superconductivity in M, hence inducing a shorter PL for increasing temperature. A $1/T$ ^{10,13,14} and $1/\sqrt{T}$ ^{10,13,14} temperature dependence of the proximity length is predicted for ballistic and diffusive systems, respectively. However, no experiments have been reported so far which scrutinize these prediction from theory on the nanoscale.

In this Letter we report experimental results on the temperature dependence of the proximity length at a S–M junction by spatially-resolved STS measurements. Our system consists of superconducting Pb islands on a 1–2 atomic layers thin metallic Pb/Ag wetting layer (WL) on Si(111). The experiments are performed with both metallic W and with superconducting Nb tips.

^aElectronic mail: sander@mpi-halle.mpg.de



Measurements with a W-tip show an apparent decrease of the PL with increasing temperature. However, experiments with a Nb-tip reveal a constant PL of 17 ± 3 nm in the temperature range 0.38–1.8 K. Our analysis suggests that thermal broadening of the occupation of electronic states of the tip is responsible for the observed temperature dependence found for the metallic tip, and this can be misinterpreted as the temperature dependence of the PL. We ascribe the observation of a constant PL to the highly diffusive character of the ultrathin metallic Pb/Ag layer, where scattering at the interfaces plays a dominant role, and intrinsic temperature effects are comparably weak. Our results identify the crucial role of the tip material for STM applications in the study of temperature effects in superconductivity.

All experiments presented here were performed under ultrahigh vacuum with a ^3He -cooled STM (for description see Ref. 9 and 15). For STM/STS measurements electrochemically etched W and Nb-tips were used. The tunneling conductance spectra (dI/dV) were acquired using a lock-in technique with a RMS modulation amplitude of $20 \mu\text{V}$ at frequency of 270 Hz.

The Pb/Ag/Si(111) sample was prepared *in-situ* by subsequent evaporation of Ag and Pb on the Si(111)- 7×7 substrate (details of the preparation can be found in Ref. 15). A non-superconducting two atomic-layer thin WL was obtained by subsequent deposition of Ag at 770 K, followed by room temperature deposition of Pb on the Si(111) substrate. Pb islands were prepared by evaporation of Pb onto the WL at 240 K, without further annealing. Figure 1(a) presents a 3D image of a constant-current STM image of a 11 monolayer (ML) high Pb island on the Pb/Ag wetting layer. Here, 1 ML corresponds to a layer thickness for Pb(111) of $d_{\text{Pb}(111)} = a_{\text{Pb}}/\sqrt{3} = 0.286 \text{ nm}$.¹⁹

In order to characterize the superconductivity of the Pb island we measure the differential conductance spectra (dI/dV) as a function of temperature [Fig. 1(g) for 0.38 K and 1.8 K] close to the island edge [black circle in Fig. 1(a)], and we extract the values of the superconducting gap $\Delta_{\text{island}}(T)$, as shown in Fig. 1(b), from a fit of the differential conductance.¹⁷ From this analysis we extrapolate an energy gap at 0 K of $\Delta_{\text{island}}(0) = 1.24 \pm 0.03 \text{ meV}$ and a critical temperature of $T_C = 6.4 \pm 0.1 \text{ K}$. These values are in good agreement with previous studies on superconducting Pb islands.^{7,8,18,20,21}

To study the temperature dependence of the superconducting proximity effect, we measure differential conductance spectra as a function of position from the Pb island into the WL for different temperatures from 0.38 to 6 K. Figures 1(c) to 1(f) show color-coded 2D plots of the differential conductance spectra as a function of position, where $x = 0$ identifies the island edge at half height. Figures 1(c) and 1(e) present measurements taken along the green line in Fig. 1(a) with a metallic W-tip at 0.38 and 1.8 K, respectively. Figures 1(d) and 1(f) present the results obtained with a superconducting Nb-tip at the same temperatures. A selection of spectra at different positions from the edge for the two tips are presented in Figs. 1(g) and 1(h). Note that all spectra are normalized to the value of the conductance measured at 5 mV bias voltage. Measurements with the W-tip show at the lowest temperature of 0.38 K [Fig. 1(g)] a fully developed superconducting gap, where the normalized zero bias conductance (NZBC) is zero in the spectrum on the Pb island. The spectra are spatially homogeneous over the island area [Fig. 1(c), $x < 0$]. Moving away from the island edge into the WL, the superconducting gap becomes smaller and the NZBC gradually increases. Finally, around 40 nm from the edge the dI/dV spectra show a shallow dip [Fig. 1(g)]. At 1.8 K the gap in the differential conductance spectra smears out, and it decays on a shorter distance of 20 nm [Fig. 1(e)].

Spectra taken with the superconducting Nb-tip show [Fig. 1(h)] a wider gap and two sharp and intense peaks at bias $V_{\text{peak}} = \pm 2.6 \text{ meV}$. This spectral shape is spatially uniform on the island and it is ascribed to tunneling between two superconductors, tip and sample. The peaks identify therefore a BCS density of states with a width given by the sum of two energy gaps $E_{\text{peak}} = \pm(\Delta_{\text{tip}} + \Delta_{\text{island}})$.^{12,22} Close to the S–M interface, we observe a proximity region where the spectra evolve from a broad gap ($\Delta_{\text{tip}} + \Delta_{\text{island}}$), to the spectra characterized by a narrower gap Δ_{tip} , ascribed to the superconducting tip [green line in Fig. 1(h)]. Our data indicate an energy gap of the tip $\Delta_{\text{tip}} = 1.40 \pm 0.05 \text{ meV}$. This compares favorably with the energy gap of bulk Nb of $1.45 \pm 0.05 \text{ meV}$.¹²

To evaluate the PL in the WL we analyze the normalized ZBC value (NZBC)^{1,6} as a function of position.⁹ Figure 2(a) shows the NZBC as a function of the distance from the Pb island for different

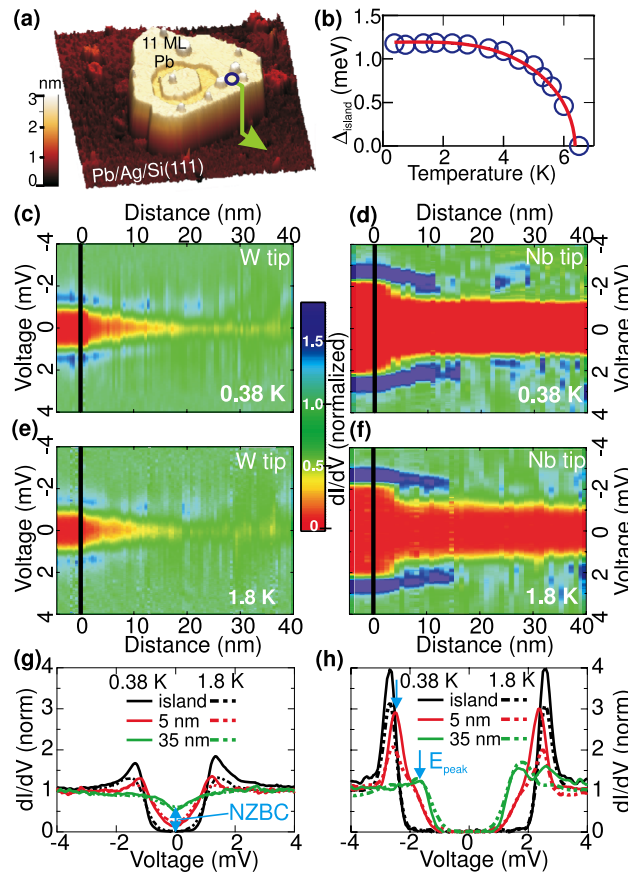


FIG. 1. (a) Constant-current STM image ($300 \times 300 \text{ nm}^2$) of a 11-ML-high Pb island on a Pb/Ag/Si(111) wetting layer. The STM image was taken at $V_{\text{bias}} = 100 \text{ mV}$ and $I = 200 \text{ pA}$. The green arrow indicates the line along which the spatial-dependent spectroscopy was performed. (b) shows the superconducting gap Δ_{island} as a function of temperature; the solid red line is a fit from the BCS density of states.¹⁶ Δ_{island} is obtained by fitting the dI/dV by the Dynes function,¹⁷ which combines a BCS density of states with a life-time broadening parameter Γ . An additional broadening due to voltage modulation and instrumental effects is considered by a convolution with a Gaussian function of width σ .^{8,18} Color-coded spatial dependence of the normalized differential conductance spectra, measured from the Pb island to the WL at 0.38 K and 1.8 K with the metallic (W) tip - Figs.(c), (e) and with the superconducting (Nb) tip - Figs.(d) and (f). The color code represents the normalized differential conductance value. The dark purple, yellow and red colors indicate low, normal and enhanced differential conductance, respectively. (g) and (h) Selected local tunneling spectra measured at 0.38 K (solid lines) and at 1.8 K (dashed lines) on the island (black) and on the wetting layer at 5 nm (red) and 35 nm (green) away from the edge.

temperatures. Up to 2.3 K, the NZBC on the island remains close to zero. With increasing temperature, the NZBC in the island reaches the value of 0.75 at 6 K. For all measurements the NZBC remains constant in the island up to the edge, and it increases monotonically on the WL side. The variation of the NZBC with position changes with temperature. We extract the PL from $\text{NZBC}(x)$ by fitting an exponential function $A + Be^{-x/\gamma_{\text{exp}}^{\text{NZBC}}}$.⁹ We plot the decay constant $\gamma_{\text{exp}}^{\text{NZBC}}$ as a function of temperature in Fig. 2(b). Starting from $21 \pm 2 \text{ nm}$ at 0.38 K, $\gamma_{\text{exp}}^{\text{NZBC}}$ decreases monotonically with temperature towards $\gamma_{\text{exp}}^{\text{NZBC}} = 3 \text{ nm}$ at 6 K. Interestingly, $\gamma_{\text{exp}}^{\text{NZBC}}$ decreases steeply by a factor 4 in the temperature range 0.38–2.3 K, where both the NZBC at the island edge and Δ_{island} remain fairly constant.

Why does the induced superconductivity in the WL decay, while Δ_{island} of the superconducting Pb island is almost constant? For the first time this phenomenon was discussed theoretically by de Gennes and co-workers.^{10,13,14} In the framework of this theory Cooper pairs can penetrate the metal over a distance which depends on several factors: the atomic order, presence of impurities in the metal, and temperature. This semi-classical picture has been widely used in literature to account for

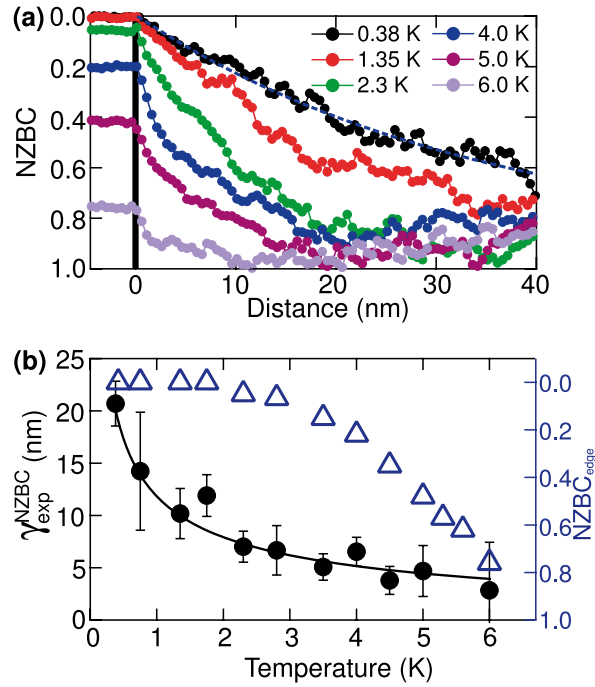


FIG. 2. (a) Normalized zero bias conductance (NZBC) as a function of distance measured with a W-tip at different temperatures. Notice that the NZBC axis counts positive downwards. The solid line is an exponential fit of the NZBC. This fitting procedure gives the decay constant $\gamma_{\text{exp}}^{\text{NZBC}}$ at 0.38 K. (b) Decay constant $\gamma_{\text{exp}}^{\text{NZBC}}$ (•, left scale) together with the normalized zero bias conductance $\text{NZBC}_{\text{edge}}$ measured at the edge of the island (Δ , right scale) as a function of temperature. The experimental data do not reach zero due to the ‘shadow effect’ (see supplemental information of Ref. 7).

the observed phenomena in literature.^{1,2,4,5,7,8,23,24} In ‘clean’ metals, i.e. no impurities, Cooper pairs sustain a diffusion over the thermal coherence length $\xi_{M,C} = \hbar v_F / (2\pi k_B T)$ (v_F - electron velocity at the Fermi energy).¹³ In presence of impurities or due to a high degree of disorder, scattering processes limit the penetration length of the Cooper pairs. In this case, the mean free path of electrons l is shorter than $\xi_{M,C}$, and this is called the ‘dirty limit’, and the proximity length in M is given by $\xi_{M,D} = \sqrt{\hbar D} / 2\pi k_B T$, with the diffusion coefficient $D = v_F l / 3$.^{13,14}

The quantitative analysis of the T-dependent data of Fig. 2(b) by a fit of $A + B/T^\kappa$, where κ is a fitting parameter, gives $\kappa = 0.55 \pm 0.07$, which points to the $1/\sqrt{T}$ dependance. One might be tempted to conclude that electron diffusivity is the decisive factor determining the PL in case of our experiments. If this was a valid statement, then we should observe the same behavior for measurements with a superconducting tip. However, measurements performed with a superconducting Nb-tip [Figs. 1(d) and 1(f)] show a completely different dependence, which questions this conclusion.

The analysis of the results obtained with the superconducting tip is based on the spatial variation of the peak energy E_{peak} ⁸ [Fig. 3(a)], as here the NZBC remains constant at zero, due to the superconducting tip. E_{peak} remains constant within the island area for both temperatures. Moving away from the island, the peak energy E_{peak} changes with increasing distance from the island edge, and it reaches 1.6 meV at the distance of 40 nm. Fitting with the exponential function gives approximately the same value of $\gamma_{\text{exp}}^{\text{peak}} = 17 \pm 3$ nm for both temperatures. This result differs from that obtained for the corresponding analysis for the metallic W-tip [Fig. 3(b)], where a pronounced change of the decay constant with temperature is observed. Our analysis for the W-tip gives $\gamma_{\text{exp}}^{\text{peak}} = 16.8 \pm 2.6$ nm and 12.0 ± 3 nm at 0.38 K and 1.8 K, respectively. A comparison of the decay constant for both tips is presented in Fig. 3(c). Studies with the superconducting tip show no clear temperature effect in the temperature range where measurements with a W-tip suggest erroneously a strong temperature dependence of the proximity length. This behavior suggests that the intrinsic effect of the temperature on the PL may be disguised by a tip effect.

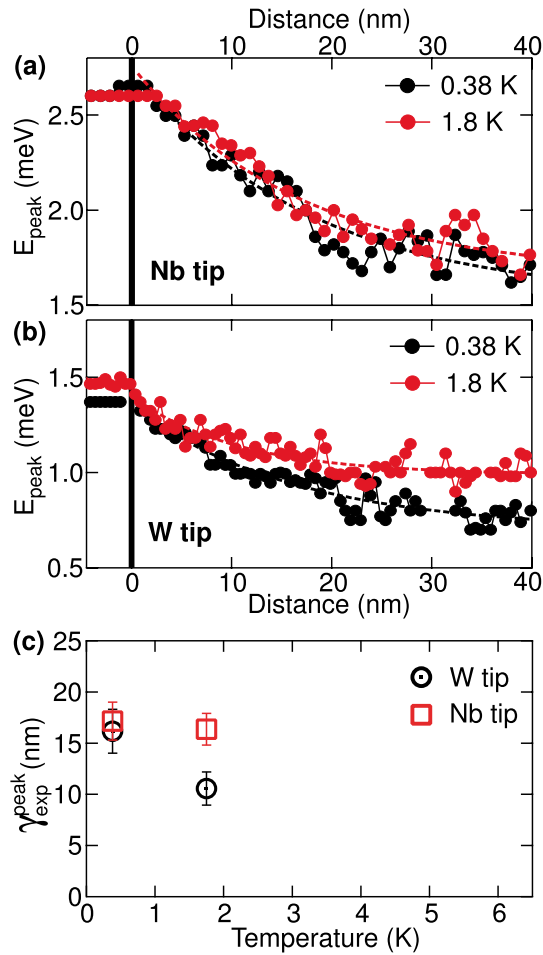


FIG. 3. Energy peak position as a function of distance obtained at 0.38 K (●) and 1.8 K (●) for (a) the superconducting Nb-tip and (b) the W-tip. (c) Decay constant $\gamma_{\text{exp}}^{\text{peak}}$ as a function of temperature for the metallic W and superconducting Nb tip.

We ascribe the observed $1/\sqrt{T}$ behavior of the PL in measurements with a metallic W-tip to thermal broadening affecting the occupation of electronic states in the tunneling process with a metallic tip.^{12,25,26} At finite temperatures, the conductance measures a density of states smeared by $\pm 2k_{\text{B}}T$ in energy, due to the width of the exponential tail of Fermi function.^{12,25,26} A smearing of the energy gap observed in tunneling experiments shows up more pronouncedly in spectra measured on a system characterized by a gap size of the same order of $\sim 4k_{\text{B}}T$. This condition is always found at every temperature in M at larger distance from S. Erroneously, the resulting change of the spectral shape can be mistaken for a temperature dependence of the PL when a metallic tip is used.

This claim is supported by calculations of the T-dependence of the differential conductance in the framework of the Usadel theory for diffusive systems, where the mean free path of electrons is short.^{1,2,6-8,11,24,27} For simplicity we apply the Usadel equation as given for 0 K. A self-consistent description within a quasiclassical description goes beyond the scope of this work, and we refer to a corresponding review [Belzig *et al.*, Superlattices and Microstructures 25, p1251 (1999)²⁸]. We calculate the DOS of the metallic WL and then apply a convolution with the derivative of the Fermi function, to simulate the tunneling process at finite temperature and obtain the differential conductance spectra. To investigate the influence of the thermal effects on the differential conductance spectra as a function of position on the Pb/Ag wetting layer we use an analytical solution obtained for a one-dimensional superconductor (S)–metal (M) system as reported by Belzig and co-workers.²⁷ This solution provides a formula which gives the DOS as a function of energy and distance from the S–M boundary. We treat the Pb island as an ideal superconducting reservoir with

a constant energy gap Δ_{island} up to the island edge, whereas on the metallic WL we assume the energy gap is zero, $\Delta_{\text{WL}} = 0$.⁷ Without any further pair-breaking mechanism, the proximity length in the WL depends on energy as $\sqrt{\hbar D/E}$, where D is the diffusion coefficient in M.^{7,8,27} This description assumes that the proximity length is uniquely given by the electronic properties of the WL. To mimic the effect of the temperature on the tunneling process and to simulate the differential conductance spectra we convolute the DOS of the WL with the derivative of the Fermi function $\partial f(T, E)/\partial E$, under the assumption of flat density of states of the tip.^{8,18,25}

$$\frac{dI}{dV}(V, x) \propto - \int_{-\infty}^{\infty} n(E, x) \frac{\partial f(T, E - eV)}{\partial E} dE. \quad (1)$$

The derivative $\partial f/\partial E$ is a bell-shaped function with width $\sim 4k_{\text{B}}T$ and unit area under the curve. For $T \rightarrow 0$, the differential conductance is directly proportional to the DOS of the superconductor. At finite temperatures however the differential conductance gives information on a thermally broadened occupation of states.^{25,26} We also include an experimental Gaussian broadening $\sigma = 0.18$ mV, which characterizes our experimental setup. The remaining parameter is the diffusion constant D in the WL. We fit D so as to reproduce the spatial dependence of the ZBC at 0.38 K.⁷ We obtain the best fit for a diffusivity of $D = 1$ cm²/s, which is more than order of magnitude smaller than in typical metals.^{1,4,7,8} In the language of diffusion in bulk metals, this suggests a highly disordered system. We assume a constant D throughout the whole temperature range, since for disordered ultrathin films the main source of electron scattering are the interfaces and structural defects.²⁹

Our spectra reveal a small dip far from the Pb island edge, as shown in Fig. 1(g), which is a signature of the electronic properties of the wetting layer. In our calculations the presence of the small dip in the WL is mimicked by a constant function $|E|^{\alpha}$, where E is the energy.^{30,31} The DOS in the M far away from the island is modified and is given by $n_0 = |E|^{\alpha}$. The parameter α is extracted from the fit of the experimental differential conductance spectra in the WL 50 nm away from S, and we obtain $\alpha = 0.14 \pm 0.02$.

Results of the calculations are presented in Fig. 4. The calculated differential conductance spectra as a function of position is shown in Fig. 4(a). Distance ‘zero’ refers to the edge of the island at half step height. We simulate spatially-resolved $\frac{dI}{dV}$ spectra for the temperatures of the measurements. Next, we proceed with the same analysis employed for the experimental results: we extract the normalized ZBC as a function of distance as is shown in Fig. 4(b) and we perform an exponential fit. In Fig. 4(c) the calculated (γ_{calc} ; green diamonds) and experimental ($\gamma_{\text{exp}}^{\text{NZBC}}$; black dots) decay constant as a function of temperature is shown. We observe that the trend of the computed γ_{calc} is in qualitative agreement with the experimental data $\gamma_{\text{exp}}^{\text{NZBC}}$, shown in Fig. 4(c). The temperature in our calculations is included by the temperature dependence of the energy gap of the island Δ_{island} and by the convolution of the DOS with the derivative of Fermi function, which accounts for thermal smearing in the tunneling process, and a very favorable description of the experimental data is obtained. This suggests that thermal broadening of the occupation of the electronic states of the tip is an important contribution to the observed temperature effect.

The question arises what is the intrinsic temperature dependence of the PL? Here we investigate an ultrathin two atomic-layer metal connected to a superconducting nanoisland. We expect that here the main source for electron scattering is scattering from the boundaries of the layers,²⁹ resulting in an extremely short electron mean free path of order several Angstroms. We speculate that with increasing temperature the highly diffusive motion of electrons may induce a temperature dependence of the PL. However, due to the dominant role of scattering at the interfaces, the PL is strongly reduced and a temperature effect is suppressed in our example. This view is corroborated by the measurements with a superconducting tip, where a constant PL is observed upon temperature variation.

In conclusion, we have studied the effect of temperature on the superconducting proximity length by scanning tunneling spectroscopy. We find no difference in the proximity length at 0.38 and 1.8 K in measurements with a superconducting Nb-tip. In the case of ultrathin films studied here scattering at interfaces is dominant, and this is the major factor which reduces the effective Cooper pair penetration length. This example shows that at reduced dimensions on the nanoscale venerable

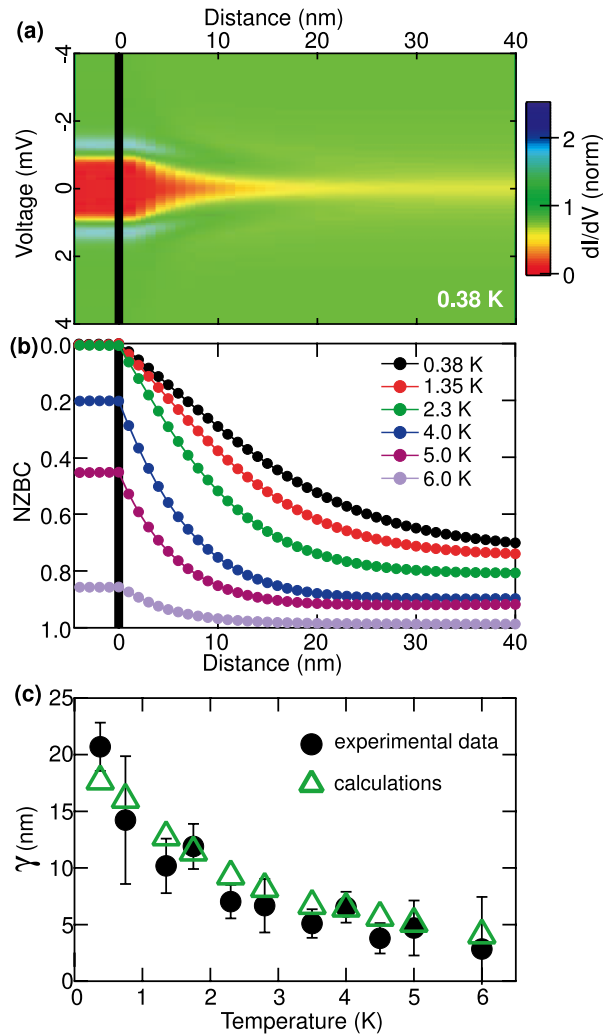


FIG. 4. (a) Computed color-coded spatial dependence of the normalized differential conductance spectra from the Pb island edge to the WL at 0.38 K. Red, yellow and purple colors indicate low, normal and enhanced differential conductance, respectively. (b) The normalized zero bias conductance (NZBC) as a function of distance at different temperatures. The NZBC axis counts positive downwards. (c) Decay constant γ as a function of temperature. Black dots (\bullet) indicate experimental data $\gamma_{\text{exp}}^{\text{NZBC}}$, the green triangles (\triangle) correspond to a calculated γ_{calc} .

concepts of the proximity effect in superconductivity and its temperature dependence need to be applied with caution.

ACKNOWLEDGMENTS

Partial financial support by DFG SFB 762 is gratefully acknowledged.

- ¹ S. Guéron, H. Pothier, N. O. Birge, D. Esteve, and M. H. Devoret, "Superconducting proximity effect probed on a mesoscopic length scale," *Phys. Rev. Lett.* **77**, 3025–3028 (1996).
- ² N. Moussy, H. Courtois, and B. Pannetier, "Local spectroscopy of a proximity superconductor at very low temperature," *Europhys. Lett.* **55**, 861 (2001).
- ³ W. Escoffier, C. Chapelier, N. Hadacek, and J.-C. Villégier, "Anomalous proximity effect in an inhomogeneous disordered superconductor," *Phys. Rev. Lett.* **93**, 217005 (2004).
- ⁴ H. le Sueur, P. Joyez, H. Pothier, C. Urbina, and D. Esteve, "Phase controlled superconducting proximity effect probed by tunneling spectroscopy," *Phys. Rev. Lett.* **100**, 197002 (2008).
- ⁵ M. Wolz, C. Debuschewitz, W. Belzig, and E. Scheer, "Evidence for attractive pair interaction in diffusive gold films deduced from studies of the superconducting proximity effect with aluminum," *Phys. Rev. B* **84**, 104516 (2011).

- ⁶ J. Kim, V. Chua, G. A. Fiete, H. Nam, A. H. MacDonald, and C.-K. Shih, "Visualization of geometric influences on proximity effects in heterogeneous superconductor thin films," *Nat. Phys.* **8**, 464–469 (2012).
- ⁷ L. Serrier-Garcia, J. C. Cuevas, T. Cren, C. Brun, V. Cherkez, F. Debontridder, D. Fokin, F. S. Bergeret, and D. Roditchev, "Scanning tunneling spectroscopy study of the proximity effect in a disordered two-dimensional metal," *Phys. Rev. Lett.* **110**, 157003 (2013).
- ⁸ V. Cherkez, J. Cuevas, C. Brun, T. Cren, G. Menard, F. Debontridder, V. Stolyarov, and D. Roditchev, "Proximity effect between two superconductors spatially resolved by scanning tunneling spectroscopy," *Phys. Rev. X* **4**, 011033 (2014).
- ⁹ M. Caminale, A. A. Leon Vanegas, A. Stępnik, H. Oka, D. Sander, and J. Kirschner, "Threshold of magnetic field response of the superconducting proximity effect for ultrathin pb/ag metallic film," *Phys. Rev. B* **90**, 220507.
- ¹⁰ P. de Gennes, *Superconductivity of Metals and Alloys* (W.A. Benjamin Inc., New York, 1966).
- ¹¹ K. D. Usadel, "Generalized diffusion equation for superconducting alloys," *Phys. Rev. Lett.* **25**, 507–509 (1970).
- ¹² W. Buckel and R. Kleiner, *Superconductivity Fundamentals and applications* (Wiley-VCH Verlag GmbH and Co. KGaA, Weinheim, 2004).
- ¹³ G. Deutscher and P. de Gennes, in *Superconductivity*, edited by R. Parks (Marcel Dekker Inc., New York, 1996).
- ¹⁴ P. G. De Gennes, "Boundary effects in superconductors," *Rev. Mod. Phys.* **36**, 225–237 (1964).
- ¹⁵ A. Stępnik, A. Leon Vanegas, M. Caminale, H. Oka, D. Sander, and J. Kirschner, "Atomic layer superconductivity," *Surface and Interface Analysis* **46**, 1262 (2014).
- ¹⁶ J. Bardeen, L. N. Cooper, and J. R. Schrieffer, "Theory of superconductivity," *Phys. Rev.* **108**, 1175–1204 (1957).
- ¹⁷ R. C. Dynes, V. Narayanamurti, and J. P. Garno, "Direct measurement of quasiparticle-lifetime broadening in a strongly-coupled superconductor," *Phys. Rev. Lett.* **41**, 1509–1512 (1978).
- ¹⁸ C. Brun, I.-P. Hong, F. m. c. Patthey, I. Y. Sklyadneva, R. Heid, P. M. Echenique, K. P. Bohnen, E. V. Chulkov, and W.-D. Schneider, "Reduction of the superconducting gap of ultrathin pb islands grown on si(111)," *Phys. Rev. Lett.* **102**, 207002 (2009).
- ¹⁹ M. Hupalo and M. C. Tringides, "Ultrafast kinetics in from the collective spreading of the wetting layer," *Phys. Rev. B* **75**, 235443 (2007).
- ²⁰ T. Nishio, T. An, A. Nomura, K. Miyachi, T. Eguchi, H. Sakata, S. Lin, N. Hayashi, N. Nakai, M. Machida, and Y. Hasegawa, "Superconducting pb island nanostructures studied by scanning tunneling microscopy and spectroscopy," *Phys. Rev. Lett.* **101**, 167001 (2008).
- ²¹ T. Cren, D. Fokin, and F. m. Debontridder, "Ultimate vortex confinement studied by scanning tunneling spectroscopy," *Phys. Rev. Lett.* **102**, 127005 (2009).
- ²² I. Giaever, "Electron tunneling between two superconductors," *Phys. Rev. Lett.* **5**, 464–466 (1960).
- ²³ J. Wang, C. Shi, M. Tian, Q. Zhang, N. Kumar, J. Jain, T. Mallouk, and M. Chan, "Proximity-induced superconductivity in nanowires: Minigap state and differential magnetoresistance oscillations," *Phys. Rev. Lett.* **102**, 247003 (2009).
- ²⁴ M. Vinet, C. Chapelier, and F. Lefloch, "Spatially resolved spectroscopy on superconducting proximity nanostructures," *Phys. Rev. B* **63**, 165420 (2001).
- ²⁵ M. Tinkham, *Introduction to superconductivity* (McGraw-Hill, Inc., New York, 1996).
- ²⁶ R. Wiesendanger, *Scanning probe microscopy and spectroscopy. Methods and applications* (Cambridge University Press, Cambridge, 1994).
- ²⁷ W. Belzig, C. Bruder, and G. Schön, "Local density of states in a dirty normal metal connected to a superconductor," *Phys. Rev. B* **54**, 9443–9448 (1996).
- ²⁸ W. Belzig, F. K. Wilhelm, C. Bruder, G. Schön, and A. D. Zaikind, "Quasiclassical green's function approach to mesoscopic superconductivity," *Superlattices and Microstructures* **25**, 1251 (1999).
- ²⁹ O. Pfennigstorf, A. Petkova, H. L. Guenter, and M. Henzler, "Conduction mechanism in ultrathin metallic films," *Phys. Rev. B* **65**, 045412 (2002).
- ³⁰ S. Levitov and A. V. Shytov, "Semiclassical theory of the coulomb anomaly," *JEPT* **66**, 214 (1997).
- ³¹ J. Kim, G. A. Fiete, H. Nam, A. H. MacDonald, and C.-K. Shih, "Universal quenching of the superconducting state of two-dimensional nanosize pb-island structures," *Phys. Rev. B* **84**, 014517 (2011).